Energy harvesting from solar and permeable pavements: A feasibility study

Domenico Vizzari[1], Pierfabrizio Puntorieri[2,]*, Filippo Praticò[3], Vincenzo Fiamma[2], Giuseppe Barbaro[2]

1. IFSTTAR, Nantes, Route de Bouaye 44344, Bouguenais, France

2. Mediterranea University DICEAM, Via Graziella, 89124 Feo di Vito – RC, Italy

3. Mediterranea University DIIES, Via Graziella, 89124 Feo di Vito – RC, Italy

puntorieri89@gmail.com

ABSTRACT. *As is well known, solar pavements are gaining more and more relevance in civil engineering due to their potential in terms of energy harvesting. This notwithstanding, several issues still hinder these typologies from getting an outstanding role, among which their uncertain durability, their surface performance (friction, drainability, texture). In the light of the above, the study described in this paper focuses on permeable and solar roadways. An innovative pavement type was designed by means of the synergistic consideration of hydraulic- and transport-related issues and performance. Once formulated and designed, the pavement underwent the preliminary feasibility study in terms of hydraulic and friction-based characteristics in order to assess its ability to perform satisfactory in dry and wet conditions. Results of the study demonstrate that the idea of coupling energy harvesting and premium properties (such as permeability) can be further developed and future research will be devoted to produce a prototype. The contributions of this study is to improve from a draining point of view the typical solar pavement structures. Results can benefit both practitioners and researchers.*

RÉSUMÉ. *Il est bien connu que les chaussées solaires s'avère pertinent dans le génie civil en raison de leur potentiel en termes de récolte d'énergie. Néanmoins, plusieurs problèmes empêchent encore ces typologies de jouer un rôle éminent, parmi lesquelles présentent leur durabilité incertaine, leurs performances de surface (frottement, capacité de drainage, texture).*

En fonction de ce qui est mentionné ci-dessus, l'étude décrite dans le présent article porte sur les chaussées perméables et solaires. Un type de chaussée innovante a été conçu en prenant en compte de manière synergique des problèmes et des performances liés à l'hydraulique et au transport. Une fois formulé et conçu, la chaussée a fait l'objet d'une étude de faisabilité préliminaire sur les caractéristiques hydrauliques et sur le frottement afin d'évaluer sa capacité à fournir des satisfactions sous les conditions sèches et humides. Les résultats de l'étude démontrent qu'il est possible de développer plus loins l'idée de coupler la récolte d'énergie et les propriétés haut de gamme (telles que la perméabilité) et que les recherches futures seront consacrées à la production d'un prototype. La contribution de cette étude est

d'améliorer d'un point de vue drainant les structures de chaussée solaires typiques. Les résultats peuvent bénéficier à la fois aux praticiens et aux chercheurs.

KEYWORDS: *solar pavement, drainability, rainfall.*

MOTS-CLÉS: *chaussée solaire, drainabilité, précipitations.*

DOI:10.3166/ACSM.42.517-534 © 2018 Lavoisier

1. Introduction

As is well known, a solar road is usually composed of three main surfaces: a road surface layer, an electronic layer and a base plate layer. The translucent and high-strength road surface layer provides traction for vehicles based on surface of texture. Sunlight passes through solar embedded collector cells, light-emitting diodes and a heating element. This layer allows handling loads and protecting the electronic layer beneath it. In several applications the electronic layer contains a microprocessor board with support circuitry for sensing loads on the surface and controlling the heating element (Duarte *et al*., 2013).

A solar road pavement usually includes three principal layers (Northmore and Tighe, 2012; Mehta *et al.*, 2015):

– A base structure in aluminium or fiberglass (Martin *et al.*, 2013) able to support the cyclic distributed load from vehicle tires without failing due to deformations, fractures, or other mechanisms. On average, it is expected that about 480 KPa is a typical design stress requirement from tires contacting the panel;

– A rubber or fiberglass layer to place the solar cells and the electronic components (Arjun *et al.*, 2011);

– A transparent layer in polycarbonate or structural glass which allows the passage of solar radiations, ensuring enough friction.

Dezfooli (Dezfooli *et al.*, 2018) proposed two different prototypes. The first one is composed of a top layer in polycarbonate for the transmission of sunlight, while the component in the middle is a rubber layer where the solar cells are placed. Finally, an aluminium plate is used to keep the layers together. The second prototype is composed of four parts including an asphalt layer to withstand the loads from the surface, two rubber layers which solar cells are embedded in and a surface porous layer to drainage the water horizontally and to protect the solar cells.

Northmore (Northmore and Tighe, 2016) developed a prototype based on the typical scheme of a solar road and it consists of three layers: a top semi-transparent layer of tempered glass having 10 mm of thickness, a fiberglass layer of 12.7 mm to allow the positioning of the solar cells, a fiberglass base of 19.1 mm able to transmit the traffic load to the subgrade.

Efthymiou (Efthymiou *et al.*, 2016) studied a photovoltaic road able to reduce the heat island effect. It is composed of a photovoltaic layer covered by a triplex security glass. The authors measured the surface temperature for several months proving that the temperatures were lower if compared to an asphalt pavement.

Yang Hongxing (2016) proposed a prototype in which solar cells are sandwiched between anti-slip tempered glass (upper layer) and support tempered glass (lower layer). The total front size is 500×500 mm and the total thickness is about 20mm. In each module, 9 monocrystalline silicon solar cells are connected in series, so that the expected power generation is about 30-40 W.

Solaroadways (solarroadways.com) is a US company which developed a hexagonal panel composed by an electrical layer (containing the solar cells) enclosed between two layer of tempered glass hermetically sealed, having an electrical output of 88-108 W/m2. Furthermore, some LED lights are embedded into the pavement (road markings).

Colas company (Colas, 2016; treevolt.com) proposed a panel containing 15-cm wide polycrystalline silicon cells that transform solar energy into electricity. The cells are coated into a multilayer substrate composed of resins and polymers, translucent enough to allow sunlight to pass through, and resistant enough to withstand truck traffic. According to Colas, 20 m2 of their system and 1000 sun-hour/year are able to provide energy for an average single French household.

Solaroad (oomspmb.com; pavegen.com) is a system which consists of concrete modules (dimensions: 2.5; 3.5 meters), with a translucent top layer of tempered glass, having a thickness of 1 cm. Underneath the glass there are crystalline silicon solar cells. The top layer has to be translucent for sunlight and able to repel dirt as much as possible. At the same time, it must be skid resistant and strong enough in order to guarantee a safe drive. The electrical output is about 3500 KWh/year per module.

Despite the above, there is lack of information about wet friction and the consequent suitability to be used in high-demanding urban and rural contexts or emergency situations (Marcianò *et al.,* 2014).

To this end, in some cases a granular surface layer is used that improves friction but implies a lower rate of solar radiation (Vizzari *et al.,* 2018).

Another important issue are flash floods which are becoming more and more relevant (Braud *et al.,* 2014; Bronstert *et al.,* 2018, Barbaro *et al.,* 2018). Climate change has a direct implication on precipitation patterns. An increase in frequency of heavy precipitation events is likely to intensify in all emission scenarios (Trenberth, 2011).

Flood is directly attributed to heavy precipitation; but climate change, rapid urbanization and unplanned urban development act like a catalyst as they modify the hydrological response of the catchment.

Flash flood is usually defined as a sudden flood in a small catchment area, occurring after a short time since the start of high intensity rainfall (Braud *et al.,* 2014). The major consequences of the flash floods occur in small basins, characterized by modest times of concentration and low storage capacity, especially if located close to urban areas. Indeed, several studies have shown that the increase of peak discharge is caused by urbanization in flood plain (Trenberth, 2011; Singha *et al.,* 2018).

As a result, it is necessary to consider how to adapt the new road systems like the solar pavement to the changing climate. Determining the best practice approach on how to adapt infrastructure to a changing climate is an ongoing challenge for the engineering community (Taylor and Philp, 2015).

The first consequence of the interaction between road systems and rainfall is the formation of a water film on the surface. The water film depth estimation is relevant in storm water management, i.e. dealing with urban drainage systems. The water depth is related to the storage dynamics on the surfaces. The distributed systems must be analysed taking into account both spatial and temporal variations (Chow *et al.,* 1988). Water film depth during intense rainstorms must be analysed also in relation to road safety problems. During storm events, unsafe water film would form if the rainwater couldn't rapidly drain, leading to potential hydroplaning phenomenon, which would considerably amplify for solar pavement. For this reason, it is necessary to design roads with elements that allow the rapid drainage of the water.

Road surface drainage refers to the drainage of water film from the road surface and the surfaces adjacent to the road formation. Several elements can be used to intercept or capture this runoff and facilitate its safe discharge to an appropriate receiving location (Road Surface and Subsurface Drainage Design, 2015).

These elements include:

– kerb and channel;

– edge and median drainage;

– table drains and blocks;

– diversion drains and blocks;

– batter drains;

– catch drains and banks;

– drainage pits.

The elements above, used to intercept or capture the runoff and facilitate its safe discharge on classic road are not enough for the new solar pavements (Dezfooli *et al.*, 2018). The purpose of this paper is to show a drainage system by applying a pipe networks, which can accelerate the drainage of rainwater on solar pavements. The behaviour of the water film on the solar pavements constituted by a pipe networks can be assimilated to that of permeable pavements.

Permeable pavements have considerably different design objectives and requirements than conventional pavements (Luis *et al.*, 2018). Their use can result in numerous storm water management and environmental benefits:

– design advances;

– infiltration performance improvements;

– potential for water reuse;

– governance and regulatory issues;

– pollution removal and water quality improvement;

– storm water management strategies and opportunities.

Studies are needed that provide a comprehensive description of the hydraulic behaviour of a permeable pavement at the field scale and that propose a general methodology for the estimation of its hydraulic parameters suggests that research is particularly needed in the development and identification of accurate physical modelling (Brunetti *et al.,* 2016).

For a better comprehension of the drainage ability of the solar pavements, it is necessary to study the behaviour of the water film and the effects of the pipe networks using a rain simulator. To this end, rain simulation and rainfall simulators are needed to learn the interaction between rainfall and road pavement in urban areas.

The advantage of using simulated rainfall is the rapid data collection under relatively uniform conditions on a pre-determined surface (Barbaro *et al.,* 2018). For accurate runoff experiments, the rainfall simulator must provide uniform rain with a proper reproduction of natural rainfall drop sizes and energies (Pérez-Latorre *et al.,* 2010). But even though rainfall simulators have been used for over 100 years in hydrology research (Wildhabera *et al.,* 2012), no general standards for the simulators exist, some examples of rainfall simulator in use are listed:

– solenoid-operated rainfall simulators, based on the original design by Miller (1987) (Miller, 1987) have been widely used to simulate rainfall with intensities ranging from 50 to 125 mm h^{-1};

– The rainfall simulator infiltrometer, that offers the advantage of low cost (Singh *et al.,* 1999);

– The Portable Wind and Rainfall Simulator (PWRS), (Fister *et al.,* 2012; Abudi and Berliner, 2012; Vardanega, 2014).

Based on the above it appears relevant to investigate techniques and method to improve friction and texture properties in order to optimize pavement performance in wet and dry conditions.

2. Objectives and paper organization

The main objectives of this paper are to study the feasibility a solar pavement from the perspective of road safety, in wet and dry conditions, including its performance in terms of drainage ability.

Based on the above, the main tasks are the following:

– study the requirements for a solar road in terms of friction, taking into account the hydroplaning effect;

– study of the expected volumes of water on the solar pavement (based on rainfall statistics in Europe) and of the solution to allow draining the rainfalls;

– design of a prototype, based on the synergistic consideration of the studies above.

Finally, conclusions are drawn and references are listed.

3. The problem of the friction in the solar roads

The prototype herein proposed differs from the ones usually set up because of the maximization of surface properties (i.e., texture and friction) through a drainage network.

This innovative structure aims at:

i) Having a better drainage. To this end the prototype has to be located on a porous asphalt and the synergetic effect of the drainability (Alvarez *et al.*, 2010; Praticò *et al.*, 2015) of the porous asphalt and the drainability of the solar pavement (through the presence of pipes) allows the rapid drainage of water.

ii) Having a higher wet friction. The aim is to reduce the probability of hydroplaning effect, breaking the water film on the top layer;

iii) Having a satisfactory structural performance. In terms of structural strength, pipes must not worsen significantly the response of pavement subject to loads (traffic loads, pressures, frequencies). In more detail, strains, stresses and deflections need to be acceptable from a structural perspective (Praticò *et al.*, 2009).

3.1. Requirements

Among the main surface requirements of pavements, the following can be listed: friction, texture, and quietness.

This section deals with friction-related properties and issues in the existing and future solar pavements.

Having glass pavement implies the necessity to study in detail surface performance and particularly:

– design friction coefficients (to use in the design of roads);

– contract specifications (usually given in terms of skid resistance, PTV, and macrotexture, SH);

– static and kinetic friction coefficients (which govern car stability during parking and successive manoeuvres);

– dependence of friction on slip percentage (because of the anti-lock braking system functioning);

– dependence of friction conditions on surface texture and tire tread depth (which affect safety and traffic operability, cf. (Vaiana and Praticò, 2014; Torbruegge and Wies, 2015).

In dry conditions, the length required to stop the car depends of the initial speed (in urban contexts, it can be supposed to have posted speeds of 50 km/h) and on friction coefficient and residual resistances (slope, aerodynamic, rolling resistance).

Actually, design values of the longitudinal friction coefficient f_l are defined in the Italian law DM 6792/2001, for different speeds (Figure 1).

For the evaluation of the texture and of the friction on existing pavements or samples (Vaiana and Praticò, 2014; Van Geffen, 2014)), CIRS specifications suggest to perform the Skid Test (through the British/portable Pendulum) to obtain the BPN (British Pendulum Number, according to CNR 105/85, now, PTV, EN 13036-4) and the sand patch test to obtain the SH (sand height, mm, CNR 94/83, corresponding in Europe to the EN 13036-1, and in the US to the ASTM E 965). The minimum values of PTV and SH requested in a new pavement are shown in Figure 2 (CIRS). Importantly, roads type E refer to the urban context.

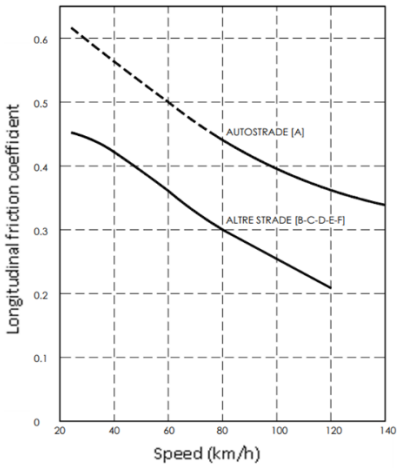

Figure 1. Design friction coefficients for different roads and speeds (DM 6792/2001)

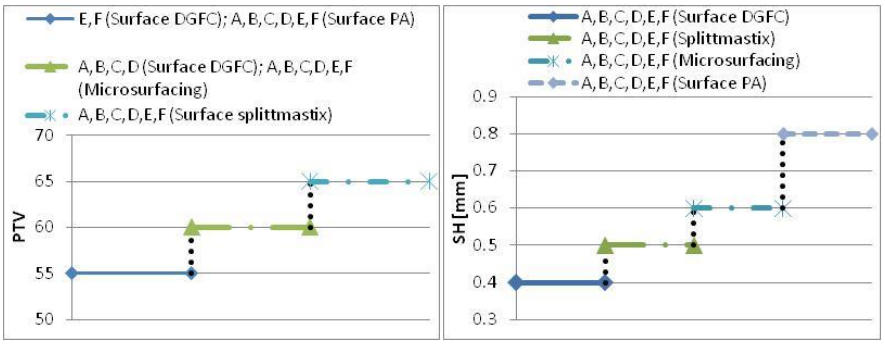

Figure 2. Lower limits of PTV (2A) and HS (2B) for different types of road and of surface (CIRS)

(A=motorways; B=main inter-urban roads; C=secondary inter-urban roads; D=urban freeways; E=Urban districts roads; F=local roads; DGFC=Dense-graded Friction Course; PA=Porous Asphalt concrete)

By referring to rubber-glass friction, three main dominions of interest can be considered:

i) static friction (e.g., car parked in a steep solar parking, Figure 3A);

ii) kinetic friction (e.g., car above starts to move, locked wheels);

iii) "real" friction (slip percentage between 0 and 100 % and car speed different from zero, Figure 3B).

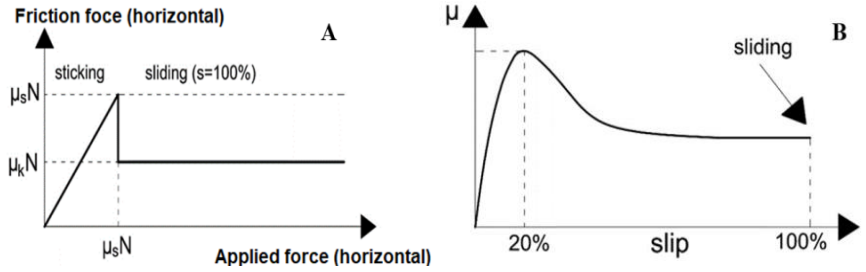

Figure 3. A: Applied horizontal force vs friction force (slip=100%); B: Friction coefficient vs slip

Static friction builds on Columb model (kshitij-iitjee.com/Forces-of-friction/) where f_{max} is the maximum friction force (parallel to the surface), N is the normal force, μs is the static friction coefficient which depends on load conditions, on temperature, and on the characteristics of surface (i.e. dry, wet, lubricated).

Table 1. Typical values of of μ_s and μ_k for different materials

Material on material	Static friction (μ_s)	Kinetic friction (μ_k)
Steel/steel	0.74	0.57
Aluminium/steel	0.61	0.47
Rubber/concrete	1.00	0.8
Glass/glass	0.94	0.4
Wood/wood	0.25-0.5	0.2
Ice/ice	0.1	0.03

If a higher (horizontal) force is applied to the car ($P>f_{max}$), the new value of friction force depends on the kinetic friction coefficient (μ_k). This latter depends on the

roughness of the surface, on the speed of sliding, on load conditions, on tire, and on the amount of lubrication.

Table 1 shows typical values of μ_s and μ_k for different materials (Ben-David and Fineberg, 2011).

For slip percentages different from 100% (wheels not locked), friction coefficient depends on slip (Figure 3B).

The longitudinal slip is defined as follows: $|s| = \left|\frac{\omega \cdot r - v}{v}\right|;\ |s| = 100\%$

where s is the slip [dimensionless], ω is the rotational speed, r is the wheel radius and v is the vehicle speed.

It is worth noting that tire-glass interaction is a very complex phenomenon (Tuononen, 2016; Localzo, 2006) and that:

i) the transition from static to kinetic friction (from sticking to sliding) does not follow exactly the one shown in Figure 3A and depends on time, N and dwell time;

ii) the peak in figure 3B is given especially in wet conditions (Tuononen, 2016; Localzo, 2006).

In wet conditions, rubber-glass hydroplaning represents an inherent risk Ervin and Balderas, 1990). There are three different types of hydroplaning: viscous, dynamic and reverted rubber hydroplaning. Viscous hydroplaning occurs when the removal of the water film from beneath the tire contact area is "resisted" by internal friction within the fluid layer. Since the viscosity of water is relatively low, this hydrodynamic component tends to dominate on thin water films. The formation of this layer can occur on smooth or macro-textured roads at any speed (Liu *et al.,* 2016; Safety Targeted Awareness Report ERA, 2013).

Dynamic hydroplaning occurs in the area of the footprint where the water depth is relatively high and in which quick changes in flow direction occur. In this phenomenon, the inertial effects of the fluid are very relevant and produce changes in momentum which cause a reaction force normal to the tire tread. Increasing speed causes an increase in the hydrodynamic pressure which provides a resulting lifting force. This latter begins at the forward edge of the footprint (Liu *et al.,* 2016). Reverted rubber hydroplaning is common for airplanes and it occurs when the locked wheel creates enough heat to vaporise the water film between rubber and pavement surface. The result is that the water trapped under the wheel turns into steam. This finally can melt the tire (Beautru *et al.,* 2012).

The dynamic hydroplaning is also influenced by water thickness, macrotexture of the road, and tire tread (Van Es, 2001). The net lifting force L [N] mentioned above is given by the following formula (Gallaway *et al.,* 1979):

$$L = \frac{1}{2} \cdot \rho \cdot v^2 \cdot S \cdot C_{LH} \tag{1}$$

Where ρ is the density of the water (998 kg/m3 for a temperature of 20°C), v is the velocity of the vehicle [m/s], S is the tire footprint area [m^2] and C_{LH} is the

hydrodynamic lift coefficient [dimensionless] (The value of C_{LH} is about 0.7 for rolling tires and 0.95 for sliding tires).

Based on equation (1), it results:

$$v = \sqrt{\frac{2}{C_{LH}\rho}p} \tag{2}$$

Where p is the pressure [Pa], v is the hydroplaning speed of the vehicle [m/s], ρ is the density of the fluid [about 1000 Ns^2/m^4]

An empirical expression to derive the hydrodynamic velocity was proposed by Gallaway (Anupan and Fwa, 2008; Praticò *et al.*, 2013):

$$v = (SD)^{0.04}(p_t)^{0.3}(TRD + 1)^{0.06}A \tag{3}$$

where:

$$A = max\left\{\left[\frac{10.409}{t_w^{0.06}} + 3.507\right]; \left[\frac{28.952}{t_w^{0.06}} - 7.817\right](MTD)^{0.14}\right\} \tag{4}$$

v is the hydrodynamic speed in mph [1mph=1.60934 kph], *SD* is the spin-down in % (SD=100% is equivalent to a locked tire), p_t is the tire pressure in psi [1psi=0.00689476MPa], t_w is the thickness of the water film in inches [1inch=25.4mm], *MTD* is the mean texture depth [inch] and *TRD* is the tire tread depth in inch/32 (Gallaway *et al.*, 1979). In the case of smooth tire and spin-down of 100% (locked tire), the expressions (3) and (4) become, respectively:

$$v = 1.084(p_t)^{0.3}A \tag{5}$$

$$A = \frac{12.639}{t_w^{0.06}} + 3.507 \tag{6}$$

Table 2. illustrates how equation (2), (3) and (5) compare.

Table 2. Hydrodynamic speed (km/h) vs. pressure eq.(1), (3) and (5)

	0.03 Mpa	**0.2 Mpa**	**0.6 Mpa**
eq (1) rolling tire	33	86	149
eq (1) sliding tire	29	74	128
eq (3)	52	92	127
eq (5)	34	61	84

In particular, equation (3) and (5) were built assuming a thickness of water film t_w=0.2mm (Kane *et al.*, 2011; Cho *et al.*, 2006), *SD*=20%, *TRD*=8mm (typical value for new tires) and *MTD*=0.55mm.

It is important to observe that viscous and dynamic hydroplaning can occur at the same time (Guzzetti *et al.*, 2001).

Consequently, considering a glass surface, the hydroplaning phenomenon becomes considerable and the project of a drainage surface represents a viable solution to prevent the creation of water films zone-1- or zone-2 related.

Further research could focus on the evaluation of the friction in dry and wet condition for solar road surfaces.

4. Feasibility study of the permeable surface

This section describes the feasibility study carried out in order to set up a solution: 1) able to decrease the risk of safety concerns in wet conditions; 2) able to improve the sustainability of the solution (cf. Kane *et al.*, 2011).

To this end, a vital issue is to estimate the maximum volume of water to manage on a solar pavement. A research on the highest rainfall recorded in Europe with a 100-year return period has been carried out.

Based on the international literature (García-Bartuala and Schneider, 2001; (Crosta and Frattini, 2003; Wieczorek and McWreath, 2001; Protecno; Wieczorek and Guzzetti, 1999; Caine, 1980; Wieczorek, 1987; Tindall, 1950; Malesińska *et al.*, 2018; Scafetta *et al.*, 2017; Cucumo *et al.*, 2018; Puntorieri *et al.*, 2017; Sheikha *et al.*, 2018) the maximum intensity in Europe corresponds to about 300 mm/h, even if thresholds usually refer to durations between 1 and 100 hr, and to intensities from 1 to 220 mm/h (Crosta and Frattini, 2003; Wieczorek and McWreath, 2001). Consequently, the value of 220-230 mm/h was used. In the case of solar pavements, the rapid drainage of the water must be carried out for two reasons:

– rapid discharge of water from surface water prevents electrical connection between the layers;

– rapid evacuation of retained water prevents the hydroplaning phenomenon.

The prototype idea is to place pipes in the solar pavement.

The input data required for dimensioning the pipes of 1 m2 of pavement are (Malesińska *et al.*, 2018):

i=230 mm/h; v_d=500 mm/s; A_{sq}=1000*1000 mm2; N=49, where i is the rainfall intensity [mm/h], v_d is the fluid flow velocity in circular pipes, and N is the number of the pipes per square meter.

The flow rate, Q, can be expressed as follows:

$$Q = i * A_{sq} = 61111{,}2\ \frac{mm^3}{s} \tag{7}$$

$$A_{dr} = \frac{Q}{v_d} = 122.2mm^2 \tag{8}$$

$$A_h = \frac{A_{dr}}{N} = 2.5\ mm^2 \tag{9}$$

$$D = \sqrt{\frac{4*A_h}{\pi}} \simeq 2\ mm \tag{10}$$

Where Q is the flow rate as function of rainfall intensity, for 1 m^2 of pavement, A_{sq} is 1 m^2 (pavement surface area, here expressed in square millimetres), A_{dr} is the area required to drainage the water, A_h is pipe cross-sectional area, and D refers to pipe diameter.

Based on the above, assuming a rainfall intensity of 230 mm/h, the diameter needed is about 2 mm and the number of pipes in the pavement is close to about 50/m^2. Finally, taking into account the pipes clogging, it is possible to hypothesize an increase in diameter of 4-6 mm. Further investigations are needed to validate this feasibility study.

5. Summary and conclusions

Solar roads represent a viable solution in terms of energy harvesting but they still present several drawbacks in terms of safety and viability when higher car speeds are requested, wet conditions are involved, and considerable longitudinal slopes may be given.

On the other hand, permeable pavements have outstanding advantages in terms of climate change mitigation, sustainability, and safety. Based on the need for a wider and safer application of solar roads, in this paper a new simple solution for the rapid drainage of water has been proposed. Moving from a typical solar road pavement, a permeable surface was designed.

The feasibility study demonstrates that, in one square meter of pavement, about 49 pipes with a diameter of about 2 mm could be able to drain a rainfall.

Further hydraulic tests will be needed to demonstrate if the estimates are correct and in order to focus on the actual ability of the system to prevent the formation of the water film and hydroplaning phenomena at least at a laboratory level.

In terms of friction, glass surface could not be the best solution, especially in wet condition anf further studies are needed in order to investigate how and if glass surfaces can offer a suitable texture level.

Consequently, future researches will concern the evaluation of the friction in wet and dry condition and the in-lab validation of the estimates above.

References

Abudi G., Berliner C. P. (2012). Rainfall simulator for field runoff studies. *Journal of Hydrology*, Vol. 454-455, No. 6, pp. 76-81.

Alvarez A. E., Martin A. E., Estakhri C. (2010). Drainability of permeable friction course mixtures. *Journal of Materials in Civil Engineering*, pp. 556-564. http://dx.doi.org/10.1061/(ASCE)MT.1943-5533.0000053

Al-Weheibi S. M., Rahman M. M. (2018). Convective heat transmission inside a porous trapezoidal enclosure occupied by nanofluids: local thermal nonequilibrium conditions for a porous medium. *Italian Journal of Engineering Science: Tecnica Italiana*, Vol. 61+1, No. 2, pp. 102-114. https://doi.org/10.1080/10407782.2017.1422632

Anupan K., Fwa T. F. (2008). Study of hydroplaning speed with variation of tire inflation pressure for smooth tire using analytical modeling. *Proceedings of the ICTI Conference.*

Arjun A. M., Ajay S., Sandhya T., Arvind V. (2011). A novel approach to recycle energy using piezoelectric crystals. *International Journal of Environmental Science and Development*, Vol. 2, No. 6. https://doi.org/10.7763/IJESD.2011.V2.175

Barbaro G., Petrucci O., Canale C. (2018). Contemporaneity of floods and storms. A case study of Metropolitan area of Reggio Calabria in Southern Italy. *Conferences New Metropolitan Perspectives*, Reggio Calabria. http://dx.doi.org/10.1007/978-3-319-92102-0_66

Beautru Y., Kane M., Tan Do M., Cerezo V. (2012). Influence of road surface microtexture on thin water film traction. *MAIREPAV7 (7th International Conference on Maintenance and Rehabilitation of Pavements and Technological Control)*. HAL Id: hal-00851131; https://hal.archives-ouvertes.fr/hal-00851131

Ben-David O., Fineberg J. (2011). Static friction coefficient is not a material constant. *Article in Physical Review Letters.* https://doi.org/10.1103/PhysRevLett.106.254301

Braud I., Bouvier C., Branger F., Delrieu G., Le Coz J., Nord G., Vandervaere J. P., Anquetin S., Adamovic M., Andrieu J., Batiot C., Boudevillain B., Brunet P., Carreau J., Confoland A., Didon-Lescot J. F., Domergue J. M., Douvinet J., Dramais G. (2014). Multi-scale hydrometeorological observation and modelling for flash flood understanding. *Hydrological and Earth System Science*, Vol. 18, No. 9, pp. 3733-3761. https://doi.org/10.5194/hess-18-3733-2014

Bronstert A., Agarwal A., Boessenkool B., Crisologo I., Fischer M., Heistermann M., Köhn-Reich L., López-Tarazón J. A., Moran T., Ozturk U., Reinhardt-Imjela C., Wendi D. (2018). Forensic hydro-meteorological analysis of an extreme flash-flood: The 2016-05-29 event in Braunsbach, SW Germany. *Science of Total Environment*, Vol. 630, pp. 977-991. https://doi.org/10.1016/j.scitotenv.2018.02.241

Brunetti G., Simunek J., Piro P. (2016). A comprehensive numerical analysis of the hydraulic behavior of a permeable pavement. *Journal of Hydrology*, Vol. 540, pp. 1146-1161. https://doi.org/10.1016/j.jhydrol.2016.07.030

Caine N. (1980). The rainfall intensity-duration control of shallow landslides and debris flows. *Geografiska Annaler*, Vol. 62A, pp. 23-27. http://dx.doi.org/10.2307/520449

Cho J. R., Lee H. W., Sohn J. S., Kim G. J., Woo J. S. (2006). Numerical investigation of hydroplaning characteristics of three-dimensional patterned tire. *European Journal of Mechanics A/Solids*, Vol. 25, No. 6, pp. 914-926. http://dx.doi.org/10.1016/j.euromechsol.2006.02.007

Chow V. T., Maidment D. R., Mays L. W. Applied Hydrology. McGraw Hill, 272 p. 1988.

Crosta G. B., Frattini P. (2003). Distributed modelling of shallow landslides triggered by intense rainfall. *Natural Hazards and Earth System Sciences*, Vol. 3, pp. 81-93. https://doi.org/10.5194/nhess-3-81-2003

Cucumo M., Ferraro V., Kaliakatsos D., Mele M. (2018). A simple correlation for the dynamic simulation of a solar thermal plant connected to a radiant floor. *Mathematical Modelling of Engineering Problems*, Vol. 5, No. 3, pp.131-138. https://doi.org/10.18280/mmep.050301

Dezfooli A. S., Nejad F. M., Zakeri H., Kazemifard S. (2017). Solar pavement: A new emerging technology. *Solar Energy*, Vol. 149, pp. 272-284. http://dx.doi.org/10.1016/j.solener.2017.04.016

Duarte F., Correia D., Ferreira A. (2013). Waynergy people: A new pavement energy harvest system. *Proceedings of the Institution of Civil Engineers: Municipal Engineer*, Vol. 166, No. 4, pp. 250-256. https://doi.org/10.1680/muen.12.00049

Efthymiou C., Santamouris M., Kolokotsa D., Koras A. (2016). Development and testing of photovoltaic pavement for heat island mitigation. *Solar Energy*, Vol. 130, pp. 148-160. http://dx.doi.org/10.1016/j.solener.2016.01.054

ERA: Wet runway-hydroplaning. Safety Targeted Awareness Report from the ERA Air Safety Group. STAR 016. March 2013.

Ervin R. D., Balderas L. (1990). Hydroplaning with lightly-loaded truck tires. *UMTRI The University of Michigan Transportation Research Institute*. http://hdl.handle.net/2027.42/867

Fister W., Iserloh T., Ries J. B., Schmidt R. G. (2012). Portable wind and rainfall simulator for in situ soil erosion measurements. *CATENA*, Vol. 91, pp. 72-84. https://doi.org/10.1016/j.catena.2011.03.002

Gallaway B. M., Ivey D. L., Hayes G. G., Ledbetter W. G., Olson R. M., Woods D. L., Schiller R. E. (1979). Pavement and Geometric Design Criteria for Minimizing Hydroplaning, Federal Highway Administration Report No. FHWA-RD-79-31, Texas Transportation, Institute, Texas A&M University.

García-Bartuala R., Schneider M. (2001). Estimating maximum expected short-duration rainfall intensities from extreme convective storms. *Physics and Chemistry of the Earth, Part B: Hydrology, Oceans and Atmosphere*, Vol. 26, No. 9, pp. 675-681. http://dx.doi.org/10.1016/S1464-1909(01)00068-5

Gerald F., Wieczoreka & Guzzetti F. (1999). A review of rainfall thresholds for triggering landslides.

Guzzetti F., Peruccacci S., Rossi M. (2017). Rainfall thresholds for the initiation of landslides in central and southern Europe. *Geomorphology*, Vol. 290, No. 3-4, pp. 39-57. https://doi.org/10.1007/s00703-007-0262-7

http://treevolt.com/

http://www.kshitij-iitjee.com/Forces-of-friction/

http://www.oomspmb.com/products/special-products-/solaroad/

http://www.pavegen.com/

http://www.solarroadways.com/

Kane M., Cerezo V., Do M. (2011). Effect of thin water film on tire/road friction. *Conference Paper*.

Liu M. W., Oeda Y., Sumi T. (2016). Modeling free-flow speed according to different water depths—From the viewpoint of dynamic hydraulic pressure. *Transportation Research Part D*, Vol. 47, pp. 13-21. https://doi.org/10.1016/j.trd.2016.04.009

Localzo A. (2006). Misura e caratterizzazione della regolarità in ambito urbano ed in particolare per le pavimentazioni lapidee della città di Napoli. UNIVERSITÀ DEGLI STUDI DI NAPOLI FEDERICO II Polo delle Scienz e e delle Tecnologie Dipartimento di Ingegneria dei Trasporti "Luigi Tocchetti". https://doi.org/10.6092/UNINA/FEDOA/3348

Malesińska A., Rogulski M., Puntorieri P., Barbaro G., Kowalska B. (2018). Displacements of the pipe system caused by a transient phenomenon using the dynamic forces measured in the laboratory. *Measurement and Control (United Kingdom)*, Vol. 51, No. 9-10, pp. 443-452. https://doi.org/10.1177/0020294018799370

Marcianò F. A., Musolino G., Vitetta A. (2014). Signal setting optimization on urban road transport networks: The case of emergency evacuation. *Safety Science*, Vol. 72, pp. 209-220. https://doi.org/10.1016/j.ssci.2014.08.005

Martín M. I., López F. A., Alguacil F. J., Romero M. (2013). Technical characterization of sintered glass ceramics derived from glass fibers recovered by pyrolysis. *Journal of Materials in Civil Engineering*, Vol. 27, No. 4, pp. 04014150. https://doi.org/10.1061/(ASCE)MT.1943-5533.0001090

Mehta A., Aggrawal N., Tiwari A. (2015). Solar roadways-the future of roadways. *International Advanced Research Journal in Science, Engineering and Technology (IARJSET) National Conference on Renewable Energy and Environment (NCREE-2015) IMS Engineering College, Ghaziabad*, Vol. 2, No. s1. https://doi.org/10.17148/IARJSET

Miller W. P. (1987). A solenoid-operated, variable intensity rainfall simulator. *Soil Science Society of America Journal*, Vol. 51, No. 3, pp. 832-834. http://dx.doi.org/10.2136/sssaj1987.03615995005100030048x

Northmore A. B., Tighe S. L. (2016). Performance modelling of a solar road panel prototype using finite element analysis. *International Journal of Pavement Engineering*, Vol. 17, No. 5, pp. 449-457. https://doi.org/10.1080/10298436.2014.993203

Northmore A., Tighe S. (2012). Innovative pavement design: are solar roads feasible? *Conference of the Transportation Association of Canada, At Fredericton.* http://dx.doi.org/10.1109/IRSEC.2013.6529704

Pérez-Latorre F. J., De Castro L., Delgado A. (2010). A comparison of two variable intensity rainfall simulators for runoff studies. *Soil and Tillage Research*, Vol. 107, No. 1, pp. 11-16. http://dx.doi.org/10.1016/j.still.2009.12.009

Praticò F. G., Moro A., Ammendola R. (2009). Factors affecting variance and bias of non-nuclear density gauges for PEM and DGFC. *The Baltic Journal of Road and Bridge Engineering*, Vol. 4, No. 3, pp. 99–107. https://doi.org/10.3846/1822-427X.2009.4.99-107

Praticò F. G., Vaiana R., Iuele T. (2015). Macrotexture modeling and experimental validation for pavement surface treatments. *Construction and Building Materials*, Vol. 95, pp. 658-666. https://doi.org/10.1016/j.conbuildmat.2015.07.061

Praticò F., Vaiana R., Giunta M. (2013). Pavement sustainability: Permeable wearing courses by recycling porous European mixes. *Journal of Architectural Engineering*, Vol. 19, No. 3, pp. 186-192. https://doi.org/10.1061/(ASCE)AE.1943-5568.0000127

Protecno, ERI S.r.l., Phoenix. Camera della pioggia.

Puntorieri P., Barbaro G., Fiamma V. (2017). Experimental study of the transient flow with cavitation in a copper pipe system. *International Journal of Civil Engineering and Technology*, Vol. 8, No. 9, pp. 1035-1041. https://doi.org/10.2495/MPF170041

Road Drainage Chapter 11: Road Surface and Subsurface Drainage Design (July 2015), State of Queensland (Department of Transport and Main Roads).

Sañudo-Fontaneda L. A., Valerio C. Andres-Valeri. (2018). The long-term hydrological performance of permeable pavement systems in Northern Spain: An approach to the "end-of-life" concept. *Water 2018*, Vol. 10, No. 4, pp. 497. https://doi.org/10.3390/w10040497

Scafetta N., Fortelli A., Mazzarella A. (2017). Meteo-climatic characterization of Naples and its heating-cooling degree day areal distribution. *International Journal of Heat and Technology*, Vol. 35, Special Issue 1, pp. S137-S144. https://doi.org/10.18280/ijht.35Sp0119Nomenclature

Singh R., Panigrahy N., Philip G. (1999). Modified rainfall simulator infiltrometer for infiltration, runoff and erosion studies. *Agricultural Water Management*, Vol. 41, No. 3, pp. 167-175. http://dx.doi.org/10.1016/S0378-3774(99)00020-7

Singha P., Sinhab V. S. P., Vijhanib A., Pahujaa N. (2018). Vulnerability assessment of urban road network from urban flood. *International Journal of Disaster Risk Reduction*, Vol. 28, pp. 237-250. http://dx.doi.org/10.1016/j.ijdrr.2018.03.017

Taylor M. A. P., Philp M. L. (2015). Investigating the impact of maintenance regimes on the design life of road pavements in a changing climate and the implications for transport policy. *Transport Policy*, Vol. 41, pp. 117-135. http://dx.doi.org/10.1016/j.tranpol.2015.01.005

Tindall R. (1950). Velocity studies in a vertical pipe flowing full. *Masters Theses.*

Torbruegge S., Wies B. (2015). Characterization of pavement texture by means of height difference correlation and relation to wet skid resistance. *Journal of Traffic and Transportation Engineering*, Vol. 2, No. 2, pp. 59-67. https://doi.org/10.1016/j.jtte.2015.02.001

Trenberth K. E. (2011). Changes in precipitation with climate change. *Clim. Res*., Vol. 47, No. 1-2, pp. 123-138. https://doi.org/10.3354/cr00953

Tuononen A. J. (2016). Onset of frictional sliding of rubber–glass contact under dry and lubricated conditions. *Scientific Reports*, Vol. 6, pp. 27951. https://dx.doi.org/10.1038%2Fsrep27951

Vaiana R., Praticò F. G. (2014). Pavement surface properties and their impact on performance-related pay adjustments, sustainability, eco-efficiency and conservation in transportation infrastructure asset management. Losa & Papagiannakis (Eds), © 2014 Taylor & Francis Group, London, ISBN 978-1-138-00147-3. http://dx.doi.org/10.1201/b16730-85

Van Es G. V. H. (2001). Hydroplaning of modern aircraft tires. *National Aerospace Laboratory NLR. NLR-TP-2001-242*

Van Geffen V. (2009). A study of friction models and friction compensation. Technische Universiteit Eindhoven. Department Mechanical Engineering Dynamics and Control Technology Group. Eindhoven. DCT 2009.118

Vardanega P. J. (2014). State of the art: Permeability of asphalt concrete. *Journal of Materials in Civil Engineering*, Vol. 26, No. 1. http://dx.doi.org/10.1061/(ASCE)MT.1943-5533.0000748

Vizzari D., Chailleux E., Lavaud S., Gennessaux E. (2018). Development of a pavement system able to capture solar energy. JTR 2018. http://doi.org/10.13140/RG.2.2.10284.56965

Wattway – Press Kit: Paving the way to tomorrow's energy. Colas 2016.

Wieczorek G. F. (1987). Effect of rainfall intensity and duration on debris flows in central Santa Cruz Mountains, California. *Geological Society of America, Reviews in Engineering Geology*, Vol. 7, pp. 93-104.

Wieczorek G. F., McWreath C. (2001). Remote rainfall sensing for landslide hazard analysis. U.S. Geological Survey OPEN-FILE REPORT 01-339. https://doi.org/10.3133/ofr01339

Wildhabera Y. S., Bänningera D., Burrib K., Alewella C. (2012). Evaluation and application of a portable rainfall simulator on subalpine grassland. *Fuel and Energy Abstracts*, Vol. 91, pp. 56-62. https://doi.org/10.1016/j.catena.2011.03.004

Yang H. X. (2016). Research and development of solar PV pavement panels for application on the green deck. final report. *The Hong Kong Polytechnic University. Renewable Energy Research Group.*

Nomenclatures

SH	Sand height test
f_l	Longitudinal friction [dimensionless]
A	Motorway
B	Main inter-urban road
C	Secondary inter-urban road
D	Urban freeway
E	Urban district road
F	Local road
DGFC	Dense-graded Friction Course
PA	Porous Asphalt
f_{max}	Maximum friction force [N]
N	Normal force [N]
μ_s	Static friction [dimensionless]
μ_k	Kinetic friction [dimensionless]
s	Slip [dimensionless]
L	Net lifting force [N]
P	Density of the water = 998 kg/m^3
v	Velocity of the vehicle [m/s]
S	Tire footprint area [m^2]
C_{LH}	Hydroplaning lift coefficient [dimensionless]
P	Pressure [Pa]
SD	Spin-down [%]

p_t	Tire pressure [psi]
t_w	Thickness water film [inch]
TRD	Tire tread depth [inch/32]
Q	Flow rate [mm^3/s]
I	Rainfall intensity [mm/h]
v_d	Fluid flow velocity in circular pipes [m/s]
N	Number of pipes
A_{sq}	Pavement surface area [mm^2]
A_{dr}	Area required to drainage the water [mm^2]
A_h	Pipe cross-sectional area [mm^2]
D	Pipe diameter [mm]